

Breathing-induced Errors in Quantification and Description of Dominant Intra-Prostatic Lesions (Dils) in PET Images: A Simulation Study by Means of The 4D NCAT Phantom

Khadijeh Bamneshin^{1,2}, Seied Rabi Mahdavi³, Ahmad Bitarafan-Rajabi^{4*}, Parham Geramifar⁵, Payman Hejazi², Majid Jadidi⁶

ABSTRACT

Background: Respiratory movement and the motion range of the diaphragm can affect the quality and quantity of prostate images.

Objective: This study aimed to investigate the magnitude of respiratory-induced errors to determine Dominant Intra-prostatic Lesions (DILs) in positron emission tomography (PET) images.

Material and Methods: In this simulation study, we employed the 4D NURBS-based cardiac-torso (4D-NCAT) phantom with a realistic breathing model to simulate the respiratory cycles of a patient to assess the displacement, volume, maximum standardized uptake value (SUV_{max}), mean standardized uptake value (SUV_{mean}), signal to noise ratio (SNR), and the contrast of DILs in frames within the respiratory cycle.

Results: Respiration in a diaphragm motion resulted in the maximum superior-inferior displacement of 3.9 and 6.1 mm, and the diaphragm motion amplitudes of 20 and 35 mm. In a no-motion image, the volume measurement of DILs had the smallest percentage of errors. Compared with the no-motion method, the percentages of errors in the average method in 20 and 35 mm- diaphragm motion were 25% and 105%, respectively. The motion effect was significantly reduced in terms of the values of SUV_{max} and SUV_{mean} in comparison with the values of SUV_{max} and SUV_{mean} in no-motion images. The contrast values in respiratory cycle frames were at a range of 3.3-19.2 mm and 6.5-46 for diaphragm movements' amplitudes of 20 and 35 mm.

Conclusion: The respiratory movement errors in quantification and delineation of DILs were highly dependent on the range of motion, while the average method was not suitable to precisely delineate DILs in PET/CT in the dose-painting technique.

Citation: Bamneshin Kh, Mahdavi SR, Bitarafan-Rajabi A, Geramifar P, Hejazi P, Jadidi M. Breathing-induced Errors in Quantification and Description of Dominant Intra-Prostatic Lesions (Dils) in PET Images: A Simulation Study by Means of The 4D NCAT Phantom. *J Biomed Phys Eng.* 2022;12(5):497-504. doi: 10.31661/jbpe.v0i0.1912-1015.

Keyword

Prostate; Signal-To-Noise Ratio; Positron-Emission Tomography

Introduction

Prostate cancer is often diagnosed as a multifocal disease, mainly spread via clones named Dominant Intra-prostatic Lesions (DILs) [1]. In patients with prostate cancer, the detection of the precise location and volume of DILs has a great impact on diagnosis and plan-

¹PhD, Department of Radiology Technology, Faculty of Allied Medical Sciences, Semnan University of Medical Sciences, Semnan, Iran

²PhD, Department of Medical Physics, School of Medicine, Iran University of Medical Sciences, Tehran, Iran

³PhD, Radiation Biology Research Center, Iran University of Medical Sciences, Tehran, Iran

⁴PhD, Echocardiography Research Center, Rajaie Cardiovascular Medical and Research Center, Iran University of Medical Sciences, Tehran, Iran

⁵PhD, Department of Nuclear Medicine, Shariati Hospital Tehran University of Medical Sciences, Tehran, Iran

⁶PhD, Department of Radiology Technology, Faculty of Allied Medical Sciences, Shahid Beheshti University of Medical Sciences, Tehran, Iran

*Corresponding author:
Ahmad Bitarafan-Rajabi
Echocardiography Research Center, Rajaie Cardiovascular Medical and Research Center, Iran University of Medical Sciences, Tehran, Iran
E-mail: bitarafan@hotmail.com

Received: 16 December 2019
Accepted: 25 May 2020

ning radiation treatment. DILs are defined by molecular or functional imaging techniques [2]. Recently, the positron emission tomography/computed tomography (PET/CT) method has been applied as a critical functional imaging tool for imaging prostate cancer, especially for detecting DILs and evaluating response to radiotherapy [3, 4]. It is now known that PET images have high-contrast with low-resolutions [5], causing some uncertainty on the determination of DIL margins.

Respiratory motion is the primary source of artifacts in PET/CT imaging, causing tumors to move rotationally and/or translationally in thorax and abdomen even at pelvis regions [6], and leading to lower maximum standardized uptake value (SUV_{max}) estimates of the region of interest and accurate quantification of the tracer uptake in tumor lesions [7, 8]. Blurring in PET imaging has been shown to reduce the amount of standardized uptake value (SUV) in lung tumors. For the correction of blurring in PET/CT images of the prostate and seminal vesicles, affected by the physiological movements of respiration and pelvic organs, it is required to know the number of variations, caused by the motion. In this investigation, we assess the respiratory movement effects on the displacement, volume, SUV_{mean} , SUV_{max} , contrast, and the SNR of DILs in frames within the respiratory cycle. Also, we used GATE [9] to obtain images and reconstruct images of DILs in PET images with high-time resolution.

Material and Methods

GATE and 4D NCAT phantom

In this simulating study, the GATE software was utilized to simulate the Siemens Biograph. ThruPoint PET/CT scanner, installed in the Diagnostic and Therapeutic Center of Tehran, Shariati Hospital.

The 4D NCAT phantom was applied to obtain CT attenuation maps and activity distribution volume as a series of transaxial slices for the pelvic organ of the human body at the

same respiratory cycle.

The 4D NCAT phantom is a sensible whole-body computer model based on non-uniform rational B-spline surfaces (NURBS), displaying the anatomy and physiology of the human body [10]. The 4D NCAT can provide high-resolution airway-gated CT datasets that realistically simulate human respiratory movement. The 4D NCAT can also establish the same breathing protocols between PET and CT. For the determination of DILs in detail, we used a pelvic activity map with the corresponding damping map to evaluate the errors due to respiratory movement in PET/CT images. For the better interpretation of PET/CT, the concentration of Gallium-68 prostate-specific membrane antigen ($^{68}\text{Ga-PSMA}$) [11] of a normal organ was obtained from the SUV measurements of previous studies [12]. Nine release and matching attenuation images were generated in a normal respiratory cycle of 5s, and thereafter, each image corresponds to 0.56 seconds per cycle (Phrase again).

In the current study, nine emission and matching attenuation images were generated in a normal respiratory cycle of 5 s and, afterwards, each image corresponded to 0.56 s per cycle (phrase again). Also, diaphragm motion amplitudes were calculated as 20 and 35 mm, which were consistent with other reported studies [13]. The matrix size for all images was 157×157 , with a pixel size of 4 mm.

DIL Size, Location, and Activity

In this study, we simulated one median DIL with a diameter size of 8 mm, placed at the right lobe of the prostate gland [14]. According to previous studies, the ratio of a DIL to the prostate activity was 8:1 in all simulations [15].

Attenuation correction and reconstruction of PET images

The 4D NCAT phantom was applied for the simulation of the human phantom of the PET scanner. GATE PET- 2- STIR platform was

used to match the GATE simulation outputs to the Software for Tomographic Image Reconstruction (STIR) to generate sinograms from the PET output roots. We used STIR to correct attenuation and reconstruction of PET images. [16]. All steps are schematically described in Figure 1. The ordered subsets expectation maximization (OSEM) algorithm, as a typically employed method in commercial reconstruction software, was performed to reconstruct the PET images, containing 4 iterations and 20 subsets. Reconstruction for each frame on a personal computer with a 3.30 GHz CPU and 14 GB of RAM took 10 min.

Evaluation the method used

The 4D NCAT generated nine emission frames and related attenuation frames. The average frame is in a normal respiratory cycle with two diaphragm motion amplitudes of 20 and 35 mm and the no-motion (no respiratory motion) emission and related attenuation frames with one lesion. The simulated PET scanner produced roots dependent on the frames. The roots were converted into sinograms and submitted to the STIR. Attenuation correction was performed for images according to the attenuation frames, which were extracted from the 4D NCAT phantom at the same respiratory motion obtained by the STIR. Images according to frames 1 to 9, and the average frame in a normal cycle and no-motion frame were produced. We assessed the magnitude of induced errors in examined DILs in terms of displacement, tumor volume, SUV_{max} , SUV_{mean} , SNR, the contrast for all phases of breathing cycle, average motion in 9 frames, and the no-motion frame. It should be noted that for the assessment of the relative errors to determine DILs in PET/CT images, the volume of DILs in the 4D NCAT

was compared with the phantom volume, and the number of variables mentioned above was compared with the values of the no-motion frame. Equation (1) was used to calculate the SUV value of a DIL, with the injected ^{68}Ga at a dose of 185 megabecquerel (MBq) and a phantom weighting 95.0 kg.

$$SUV = \frac{{}^{68}\text{Ga activity concentration (MBq/ml)}}{\text{Injected dose (MBq/phantom weight (g))}} \quad (1)$$

The SUV_{max} of a DIL was measured using the maximum amount of DIL voxel, while SUV_{mean} was calculated by means of volume of interest (VOIs) with a fixed threshold of 20%, 25%, 30%, 35% and 40% of the maximum signal intensity according to the absorption rate of ^{68}Ga -PSMA in PET images to quantitative nine frames, average (AV), and images. The change in SUV_{max} and SUV_{mean} of DIL was analyzed with respect to that of the no-motion frame by equation (2).

$$\Delta SUV_{max} = \frac{SUV_{max} - SUV_s}{SUV_s} \quad (2)$$

Where SUV_s denotes the SUV_{max} of DIL measured using the no-motion image of PET, and SUV_{max} implies values obtained from PET. For the measurement errors in estimating and localizing DIL volume, a threshold strategy was used for determining VOIs.

We used the threshold setting of 20%, 25%, 30%, 35%, and 40% of maximum voxel intensity to evaluate the optimal correlation of volume ratio of PET/CT images. For each image, a change in DIL volume with respect to that of the no-motion frame was calculated by equation (3).

$$\Delta V = \frac{V' - V_{True}}{V_{True}} \quad (3)$$

Where V_{True} is defined as the DIL volume



Figure 1: The procedures of the simulation to obtain positron emission tomography (PET) images

measured using the NCAT phantom, and V' is the DIL volume obtained by PET images. The DIL volume center voxel was used to measure respiratory displacement during the respiratory cycle. The center voxels were defined for analysis by a human expert.

Equation (4) was used to calculate the signal to noise ratio (SNR) for all images that the ratio of the mean value divided to the standard deviation (SD) in VOI.

$$SNR = \frac{Mean(VOI)}{SD(VOI)} \quad (4)$$

Moreover, equation (5) was applied to calculate the contrast value as DIL quantification.

$$Contrast = \frac{Maximum\ voxel\ value(VOI)}{Mean\ voxel\ value\ of\ background(VOI)} \quad (5)$$

Results

DIL Displacement

For all frames, the Euclidean distance to the right-left (RL), upper-lower (SI) and anterior-posterior (AP) for diaphragm movements of 20 and 35 mm are shown in the Figure 2. The displacement values in the RL direction are at a range of 0.87 to 1.07 mm. There was no significant difference of displacement in RL direction quantities of all images compared with quantities of the no-motion image.

Accordingly, in the SI direction, the maximum amount of displacement compared with the no-motion image was in frames 3 and 4, which were 3.9 mm and 6.1 mm for the diaphragm motion amplitudes of 20 and 35 mm, respectively.

The difference of displacement values in the SI direction between the average frame and no-motion image for the diaphragm motion amplitudes of 20 and 35 mm was statistically significant.

In the AP direction, maximum displacement was in frames 6 and 7 of the respiratory cycle. There was no marked difference in the amount of displacement between the average and no-motion images in the diaphragm motion amplitude of 20 mm; however, the maximum

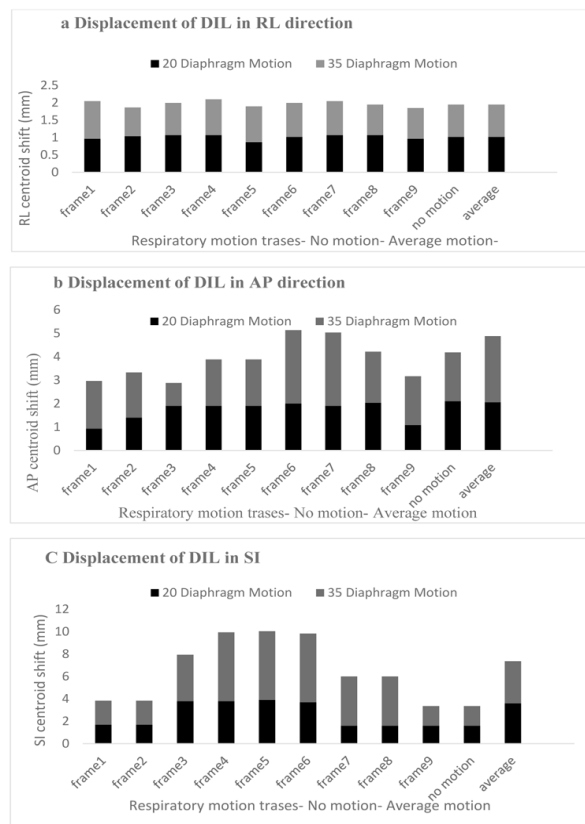


Figure 2: Displacement of Dominant Intra-prostatic Lesions (DILs) (mm) as a result of the respiratory motion in a) RL (right-left), b) anterior-posterior (AP), and c) the SI (upper-lower) direction in the respiratory motion traces, no-motion and average

difference between the average and no-motion modes was observed at diaphragm motion amplitude of 35 mm.

Calculating the volume of the Lesion

Table 1 shows the percentage of DIL volume errors in the respiratory cycle frames. DIL volumes were evaluated with thresholds at 20 %, 25%, 30%, 35%, and 40% of the maximum voxel severity of respiratory patterns. The comparison of all volumes with the constructed DIL volume showed that the volume measurement errors increased in 35 mm-diaphragm motion.

In the no-motion image, the volume mea-

Table 1: Dominant Intra- prostatic Lesion (DIL) volume errors of positron emission tomography (PET)

Frame A and B	20% max	25% max	30% max	35% max	40% max
Frame1	13	-5	-21	-23	-34
	30	2	-19	-22	-32
Frame2	27	1	-2	-16	-40
	3	46	28	0	-25
Frame3	9	-5	-16	-36	-43
	14	-5	-5	-7	-25
Frame4	9	-5	-16	-36	-43
	55	34	14	2	-5
Frame5	11	-5	-9	-3	-36
	55	34	14	2	5
Frame6	20	-5	-16	-23	-41
	18	0	-14	-16	-42
Frame7	28	-5	-16	-23	-20
	55	30	16	-2	-12
Frame8	77	39	21	0	-12
	55	30	16	-2	-12
Frame9	-5	-8	-36	-46	-57
	20	0	-12	-23	-28
No motion	13	5	-21	-23	-34
	30	2	-19	-22	-32
Average	62	25	16	-12	-19
	162	105	48	7	-9

A and B represent 20 and 35 mm diaphragm motion amplitudes

surement of DIL comprised of the smallest percentage errors. At a 20% (of the maximum) voxel intensity threshold, the estimated amount of the DIL volume in the no-motion image increased, resulting in reduced efficiency of the treatment in the dose-painting technique.

A 25% (of maximum) voxel intensity threshold would be appropriate to estimate the volume of DIL in the no-motion image, while the percentages beyond 25% (of maximum) voxel intensity threshold can underestimate the DIL volume in the no-motion image. The number of errors in the average method compared to the no-motion method in 20 and 35 mm dia-

phragm motion was 25% and 105%. Thus, there was a significant difference between the estimated volume of the average images compared to the volume of the 4D NCAT phantom.

Measured Values of SUV_{mean} and SUV_{max} in DILs

Table 2 shows the measurements of SUV_{max} and SUV_{mean} of DIL in nine frames, average frame, and no-motion frames with thresholds at 25%. The changes in SUV_{max} and SUV_{mean} were measured and analyzed for DILs by two diaphragm movement amplitudes. As shown in Table 2, the comparison of the no-movement PET image with other images indicated

Table 2: Measured Value of standardized uptake value SUV_{mean} and SUV_{max} in Dominant Intra- prostatic Lesions (DILs)

	SUV_{mean}		SUV_{max}	
	A	B	A	B
Frame1	1.51	3.10	3.90	6.47
Frame2	2.80	2.35	6.01	5.17
Frame3	3.20	3.06	7.40	6.37
Frame4	3.18	2.44	7.3	4.89
Frame5	3.45	3.01	7.89	6.71
Frame6	2.66	2.02	6.40	6.71
Frame7	2.80	2.01	5.69	4.30
Frame8	2.44	2.02	5.40	4.20
Frame9	3.30	3.07	7.80	6.90
No motion	3.53	3.01	6.47	6.47
Average	2.90	0.90	5.36	2.19

A and B represent 20 and 35 mm diaphragm motion amplitudes

SUV: Standardized uptake value

that the motion effect significantly reduced the values of SUV_{max} and SUV_{mean} in comparison with the values of SUV_{max} and SUV_{mean} in no-motion frames.

SNR and Contrast

SNR and contrast values were used to assess image quality. Table 3 depicts the measurements of SNR and contrast in 9 frames, average frame, and no- motion frame.

The contrast values in the respiratory cycle frames were at a range of 3.3 to 19.2 mm and 6.5 to 46 for diaphragm movements' amplitudes of 20 and 35 mm, respectively. According to Table 3, there was a significant difference in SNR diaphragm movement amplitudes of 35 mm between the no-motion and average frames.

Discussion

Analytical simulations with adequate modeling have notable profits and can provide validated results. The general pattern of movement of the prostate and DILs is unpredict-

able due to the respiratory and diaphragmatic movements because its repetition is influenced by the bladder movement, and the fullness of the bladder and rectum. However, the Monte Carlo simulation method has provided facilities to investigate the effect of the respiratory movement on quantitative and qualitative accuracy of the images obtained from prostate tumors. The results showed that the maximum displacement of DILs in the SI line was 3.9 and 6.1 mm in the diaphragm s amplitudes of 20 and 35 mm, respectively, which was similar to the results of a study conducted by Hong and colleagues [17]. The assessment of the mass movement in the lung and prostate during breathing and diaphragm movements was performed. To best of our knowledge, no study has been so far carried out on the extent of the mass movement during breathing and diaphragm movements [17]. The results showed that the displacement of respiratory and diaphragm movements affects the volume of DILs in different frames of the respiratory cycle and the mean respiratory motion. Our findings demonstrated that the relative volume

Table 3: Measured Values of signal to noise ratio (SNR) and Contrast

	SNR		Contrast	
	A	B	A	B
Frame1	3.10	3.30	5.90	6.50
Frame2	1.14	3.50	14.87	36.90
Frame3	1.10	3.60	18.5	42.60
Frame4	1.10	3.57	18.5	30.62
Frame5	1.15	3.57	19.2	30.60
Frame6	1.07	4.10	15.6	37.20
Frame7	1.02	3.57	13.87	28.60
Frame8	1.50	3.54	13.50	28.60
Frame9	3.10	3.30	3.30	46.00
NO motion	5.2	3.12	16.50	43.13
Average	3.40	3.04	11.60	14.60

A and B represent 20 and 35 mm diaphragm motion amplitudes

SNR: Signal to noise ratio

of DILs in comparison with the actual size of DILs in the diaphragm movement domains of 20 and 35 mm, was at a percentage range of -5-77% and 14-55%, respectively. Grammifar and colleagues have conducted a similar study on the mass of lung and liver in three phases of the respiratory motion. The percentage of relative volume changes vary between 1% and 135% depending on the size and location of the mass in the abdominal area [7].

As displayed in Table 2, the comparison of the no-motion PET image with other PET images revealed that the motion effect significantly diminished the values of SUV_{max} and SUV_{mean} compared to the values of SUV_{max} and SUV_{mean} in the no-motion image. The contrast values in the respiratory cycle frames were at a range of 3.3 to 19.2 mm and 6.5 to 46 for diaphragm motion amplitudes of 20 and 35 mm, respectively. Notably, according to Table 3, there was a significant difference in SNR diaphragm motions amplitudes when measured at 35 mm between the no-motion and average frames. The results indicated that displacement of the respiratory and diaphragmatic movements influences the volume of DILs, SUV_{mean} , and SUV_{max} , which are all crucial for the detection of DILs.

In this study, quantitative and qualitative changes in PET images in high-temporal resolution respiratory cycles were evaluated precisely, whereas previous studies failed to measure these alterations at high-temporal resolution accurately. Previous research only evaluated the tail-end and deep tail-end of the above values.

Changes are important in radiotherapy results of the Dose-painting by contours (DPC) technique. DPC is a radiotherapy technique for the better control of the mass during the treatment course and its side effects, requiring the precise determination of the location of the mass, as well as its volume and mass function for the administration of higher doses of a particular drug. Although in radiotherapy treatment planning, the motion is regarded as a

marginal determinant, sometimes the overestimation of the margins of DILs is not suitable in some therapeutic approaches, for example dose-painting techniques or intensity-modulated radiotherapy (IMRT) [18]. The enhancement of the therapeutic response through boosting DILs and maintaining the standard dose in the rest of the prostate is the aim of the external beam radiotherapy treatment, which may need the motion compensation technique to ensure detection and delineation accuracy for maximum delivery of treatments to DILs.

Conclusion

In the current study, the Monte Carlo simulation, as a reference concept, was used to assess the effects of respiration and diaphragm motion on estimating the location and volume of DILs in prostate cancer. Our proposed respiratory motion leads to the noise and blurring of PET images. Also, we showed that the volume of DILs extracted by absorbance of 25% (of maximum) voxel intensity in the threshold method was closer to authenticity compared with other examined thresholds.

Acknowledgment

This work was supported by a research grant (Number: 95043029510) provided by the Iran University of Medical Sciences.

Authors' Contribution

A. Bitarafan- Rajabi conceived and coordinated all phases of the project. Kh. Bamneshin conceived and collected images and analyzed information and wrote the article with the help of colleagues. SR. Mahdavi provided the necessary facilities and training to design the treatment with the IMRT technique. P. Geramifar helped to gather images. P. Hejazi helped in the simulation stage. M. Jadidi edited the article. All the authors read, modified, and approved the final version of the manuscript.

Ethical Approval

The Ethics Committee of Iran University of Medical Sciences approved the protocol of the study (Ethic cod: IR.IUMS.REC.1395.9221339203).

Conflict of Interest

None

References

- Cooper CS, Eeles R, Wedge DC, Van Loo P, et al. Analysis of the genetic phylogeny of multifocal prostate cancer identifies multiple independent clonal expansions in neoplastic and morphologically normal prostate tissue. *Nat Genet.* 2015;**47**(4):367-72. doi: 10.1038/ng.3221. PubMed PMID: 25730763. PubMed PMCID: PMC4380509.
- Bentzen SM. Theragnostic imaging for radiation oncology: dose-painting by numbers. *Lancet Oncol.* 2005;**6**(2):112-7. doi: 10.1016/S1470-2045(05)01737-7. PubMed PMID: 15683820.
- Wang T, Press RH, Giles M, Jani AB, et al. Multiparametric MRI-guided dose boost to dominant intraprostatic lesions in CT-based High-dose-rate prostate brachytherapy. *Br J Radiol.* 2019;**92**(1097):20190089. doi: 10.1259/bjr.20190089. PubMed PMID: 30912959. PubMed PMCID: PMC6580917.
- Cattaneo GM, Bettinardi V, Mapelli P, Picchio M. PET guidance in prostate cancer radiotherapy: Quantitative imaging to predict response and guide treatment. *Phys Med.* 2016;**32**(3):452-8. doi: 10.1016/j.ejmp.2016.02.013. PubMed PMID: 27080346.
- Foster B, Bagci U, Mansoor A, Xu Z, Mollura DJ. A review on segmentation of positron emission tomography images. *Comput Biol Med.* 2014;**50**:76-96. doi: 10.1016/j.combiomed.2014.04.014. PubMed PMID: 24845019. PubMed PMCID: PMC4060809.
- Malone S, Crook JM, Kendal WS. Respiratory-induced prostate motion: quantification and characterization. *Int J Radiat Oncol Biol Phys.* 2000;**48**(1):105-9. doi: 10.1016/s0360-3016(00)00603-9. PubMed PMID: 10924978.
- Geramifar P, Zafarghandi MS, Ghafarian P, Rahmim A, Ay MR. Respiratory-induced errors in tumor quantification and delineation in CT attenuation-corrected PET images: effects of tumor size, tumor location, and respiratory trace: a simulation study using the 4D XCAT phantom. *Mol Imaging Biol.* 2013;**15**(6):655-65. doi: 10.1007/s11307-013-0656-5. PubMed PMID: 23780352.
- Boucher L, Rodrigue S, Lecomte R, Bénard F. Respiratory gating for 3-dimensional PET of the thorax: feasibility and initial results. *J Nucl Med.* 2004;**45**(2):214-9. PubMed PMID: 14960638.
- Sheen H, Im KC, Choi Y, Shin H, et al. GATE Monte Carlo simulation of GE Discovery 600 and a uniformity phantom. *Journal of the Korean Physical Society.* 2014;**65**(11):1802-8. doi: 10.3938/jkps.65.1802.
- Segars WP, Tsui BM, Frey EC, Fishman EK. Extension of the 4D NCAT phantom to dynamic x-ray CT simulation. Nuclear Science Symposium. Conference Record (IEEE Cat. No.03CH37515); Portland, OR, USA: IEEE; 2003. doi: 10.1109/NS-SMIC.2003.1352577.
- Wang XY, Zhao YF, Liu Y, Yang YK, Zhu Z, Wu N. Comparison of different automated lesion delineation methods for metabolic tumor volume of 18F-FDG PET/CT in patients with stage I lung adenocarcinoma. *Medicine (Baltimore).* 2017;**96**(51):e9365. doi: 10.1097/MD.0000000000009365. PubMed PMID: 29390527. PubMed PMCID: PMC5758229.
- Komek H, Can C, Yilmaz U, Altindag S. Prognostic value of 68 Ga PSMA I&T PET/CT SUV parameters on survival outcome in advanced prostate cancer. *Ann Nucl Med.* 2018;**32**(8):542-52. doi: 10.1007/s12149-018-1277-5. PubMed PMID: 30006752.
- KOLÁŘ P, Neuwirth J, Šanda J, Suchanek V, et al. Analysis of diaphragm movement during tidal breathing and during its activation while breath holding using MRI synchronized with spirometry. *Physiol Res.* 2009;**58**(3):383-92. doi: 10.33549/physiolres.931376. PubMed PMID: 18637703.
- Von Eyben FE, Kiljunen T, Kangasmaki A, Kairamo K, et al. Radiotherapy boost for the dominant intraprostatic cancer lesion—a systematic review and meta-analysis. *Clin Genitourin Cancer.* 2016;**14**(3):189-97. doi: 10.1016/j.clgc.2015.12.005. PubMed PMID: 26768965.
- Khalil MM. Basic science of PET imaging. Cham: Springer International Publishing; 2017.
- Karakatsanis NA, Tsoumpas C, Zaidi H. Quantitative PET image reconstruction employing nested expectation-maximization deconvolution for motion compensation. *Comput Med Imaging Graph.* 2017;**60**:11-21. doi: 10.1016/j.compmedimag.2016.11.006. PubMed PMID: 27887989.
- Huang CY, Tehrani JN, Ng JA, Booth J, Keall P. Six degrees-of-freedom prostate and lung tumor motion measurements using kilovoltage intrafraction monitoring. *Int J Radiat Oncol Biol Phys.* 2015;**91**(2):368-75. doi: 10.1016/j.ijrobp.2014.09.040. PubMed PMID: 25445555.
- Bouchelouche K, Oehr P. Recent developments in urologic oncology: positron emission tomography molecular imaging. *Curr Opin Oncol.* 2008;**20**(3):321-6. doi: 10.1097/CCO.0b013e3282f8b02b. PubMed PMID: 18391633.